Supporting Information

A Hydrothermal Stable Zn(II)-based Metal-Organic Framework: Structural Modulation and Gas Adsorption

Xiuling Zhang,[a] Yong-Zheng Zhang,[a] Da-Shuai Zhang,[a*] Baoyong Zhu,[a] Jian-Rong Li[b*]

[a] *Key Laboratory of Coordination Chemistry, Functional Materials in Universities of Shandong (De Zhou University), De Zhou, 253023 P. R. China*

E-mail: dashuai_74@163.com

[b] *Beijing Key Laboratory for Green Catalysis and Separation and Department of Chemistry and Chemical Engineering, College of Environmental and Energy Engineering, Beijing University of Technology, Beijing 100124, P. R. China.*

E-mail: jrli@bjut.edu.cn

Table S1. Crystal data and structure refinement parameters for **1**

Empirical formula	$C_{24}H_{13}N_3O_{10}Zn_2$
Formula weight	634.11
Temperature (K)	100(2)
Crystal system	Hexagonal
Space group	$P6_3/m$
a (Å)	16.7612(16)
b (Å)	16.7612(16)
c (Å)	6.8980(9)
α (°)	90
β (°)	90
γ (°)	120
Volume(Å^3)	1678.3(3)
Z, D_c(g cm^{-3})	2, 1.255
F(000)	636
θ range (°)	5.28 to 67.06
Reflections collected	1091
Goodness-of-fit	1.124
R_1 wR_2 [$I > 2\sigma(I)$]	R_1 = 0.0711, wR_2 = 0.1992
R_1 wR_2 [all data]	R_1 = 0.0745, wR_2 = 0.2012
Largest diff. peak and hole (e/Å^3)	0.903 and -0.798

Table S2. Selected bond lengths (Å) and angles (°) for **1**

Zn(1)-O(3)	1.9493(11)	O(1)#1-Zn(1)-O(1)#2	111.15(17)
Zn(1)-O(1)#1	1.921(4)	O(1)#1-Zn(1)-O(3)	110.5(8)
Zn(1)-O(1)#2	1.921(4)	O(1)-Zn(1)-O(1)#2	111.15(17)
Zn(1)-O(1)	1.921(4)	O(1)-Zn(1)-O(3)	82.2(3)
O(1)#1-Zn(1)-O(1)	111.15(17)	O(1)#2-Zn(1)-O(3)	126.9(7)

Symmetry codes: #1-y+1, x-y, z; #2 -x+y+1, -x+1, z

IR Spectra

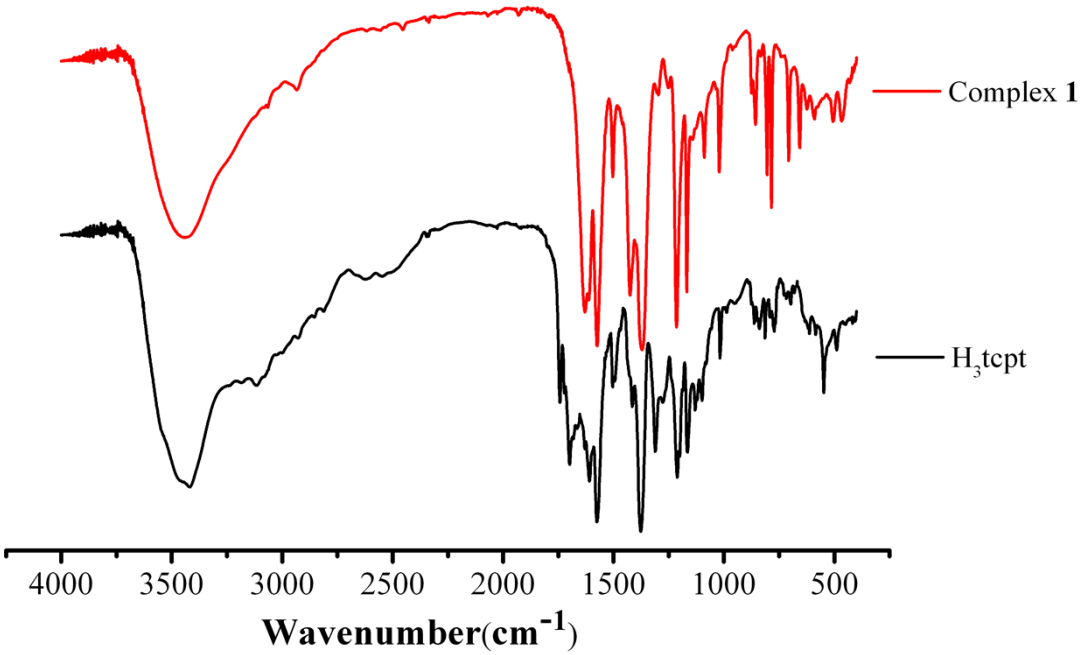

Figure S1 IR spectra of Ligand and the obtained MOF (black: Ligand (H_3tcpt); red: **1**)

PXRD and TGA

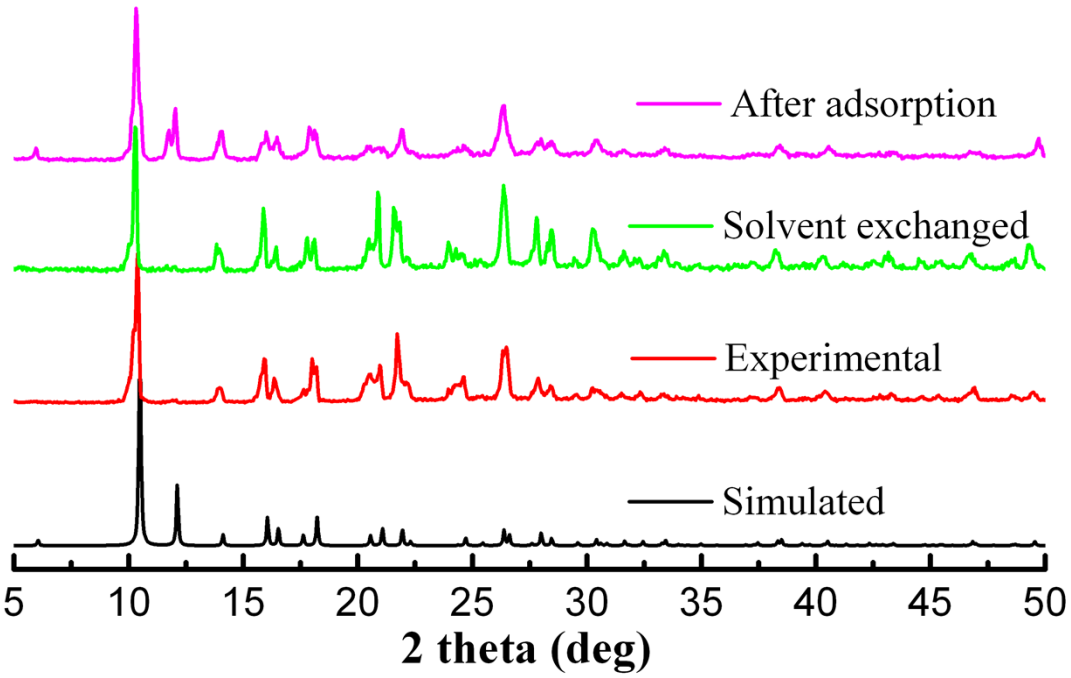

(a)

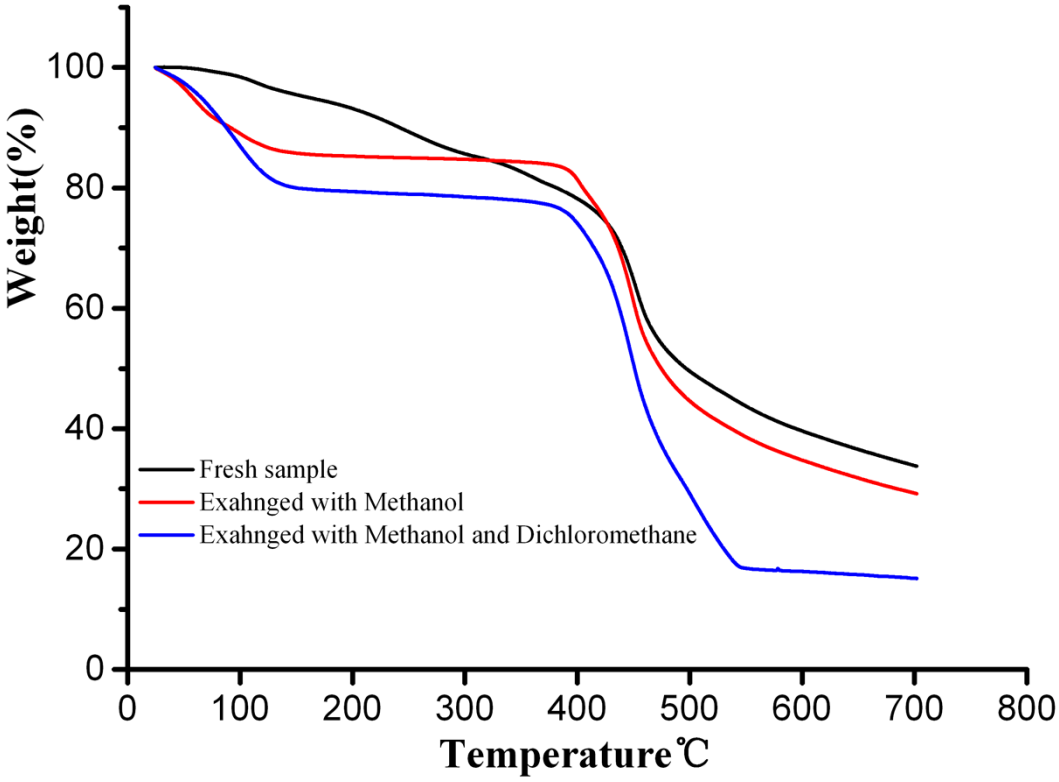

(b)

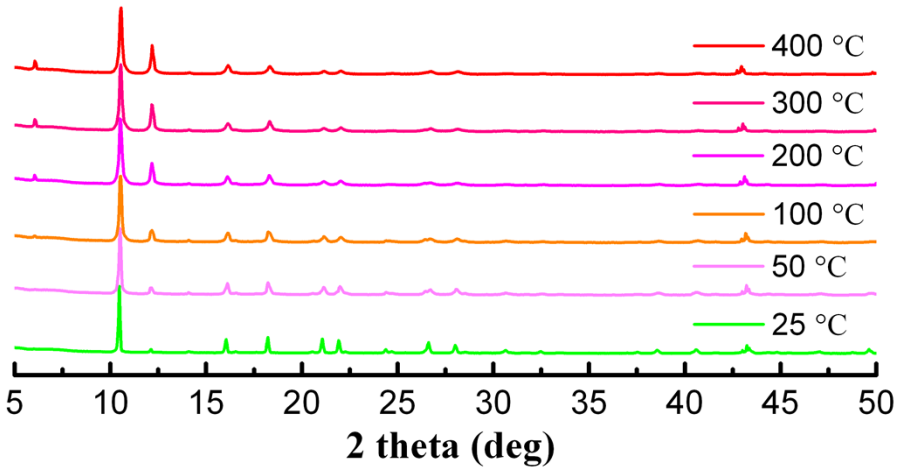

(c)

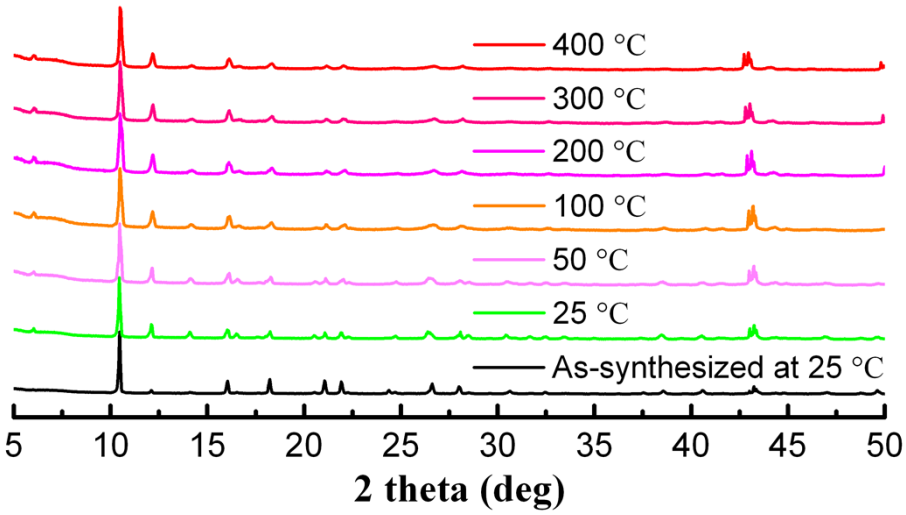

(d)

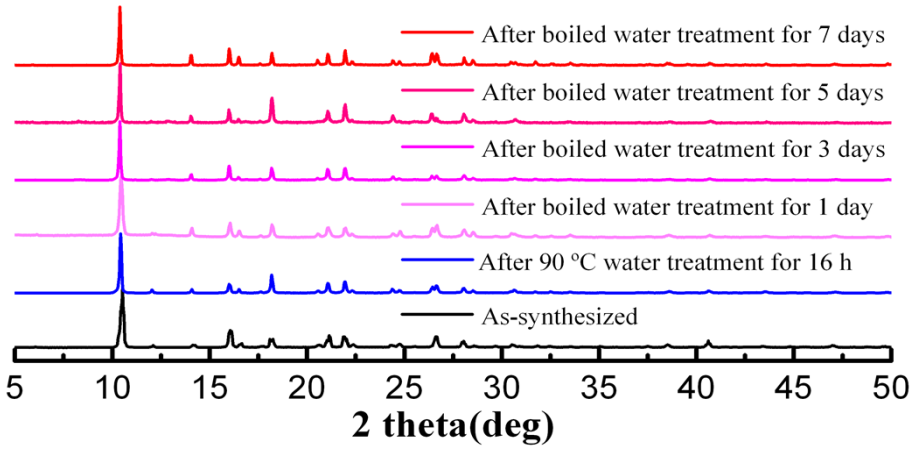

(e)

Figure S2 (a) PXRD patterns for simulated and experimental samples of **1**. (b) TGA curves of **1**. (c) Temperature-dependent PXRD patterns of as-synthesized samples of **1**. (d) Temperature-dependent PXRD patterns of activated samples of **1**. (e) PXRD patterns of **1** which has been treated by boiled water.

Isosteric Heat of Adsorption.

The isosteric heat of H_2 adsorption was estimated from the H_2 adsorption data measured at 77 K and 87 K. The data were fit to equation (1), where P is pressure (Torr), N is amount adsorbed H_2 gas (mmolg^{-1}), T is temperature (K), and a_i and b_j are temperature independent empirical parameters.

$$\ln p = \ln(N) + \frac{1}{T}\sum_{i=0}^{m} a_i N^i + \sum_{j=0}^{n} b_j N^j \quad \textbf{(1)}$$

To estimate the values of the isosteric heat of H_2 adsorption, equation (2)[S1] was applied, where R is the universal gas constant.

$$Q_{st} = -R\sum_{i=0}^{m} a_i N^i \quad \textbf{(2)}$$

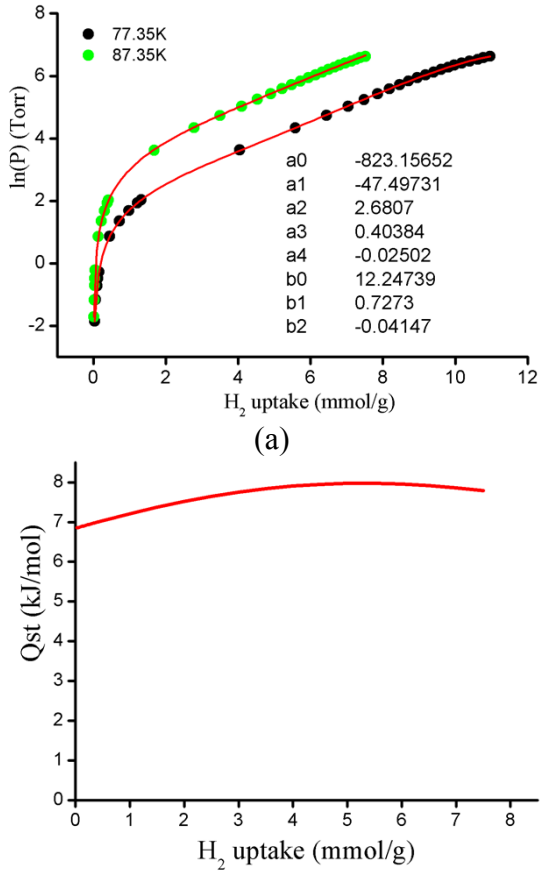

Figure S3 (a) The virial fit for the H_2 adsorption isotherms of **1** (b) Q_{st} of the H_2 adsorption for **1**

The data of the CO_2 adsorption isotherms at 273 K and 298 K, respectively, were fit to Langmuir-Freundlich equation (3),[S2] where P is pressure (kPa), N is the amount

adsorbed gas (mmolg^{-1}), N_m is the amount adsorbed gas at saturation, and b and t are constants. The isosteric heats of CO_2 and CH_4 adsorption were calculated by applying these fits to the Clausius-Clapeyron equation (eq 4),[S3] where Q_{st} is the isosteric heat of adsorption (kJmol^{-1}), P is the pressure (kPa), T is the temperature (K), R is the gas constant.

$$\frac{N}{N_m} = \frac{N_m b P^{(1/t)}}{1 + b P^{(1/t)}} \tag{3}$$

$$\frac{\partial(\ln p)}{\partial(1/T)} = \frac{Q_{st}}{R} \tag{4}$$

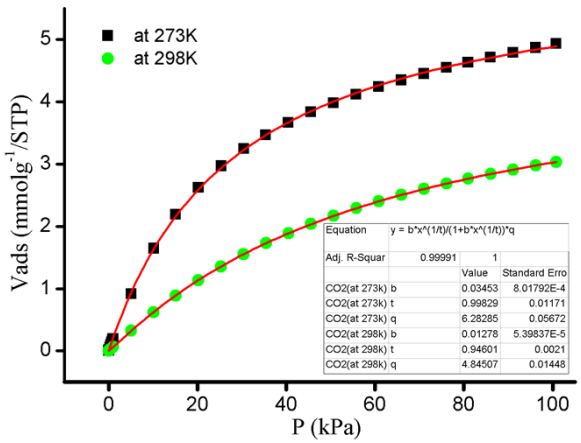

(a)

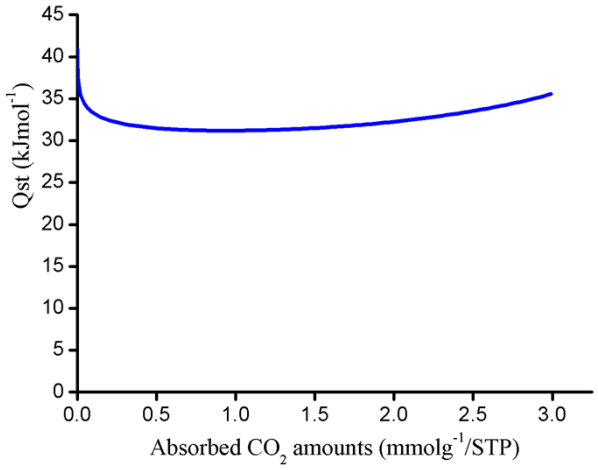

(b)

Figure S4 (a) CO_2 gas adsorption isotherms of **1** at 273 and 298 K, the red solid lines correspond to Langmuir-Freundlich equation fits. (b) Q_{st} of CO_2 for **1**.

Calculation of CO_2 Adsorption Selectivities

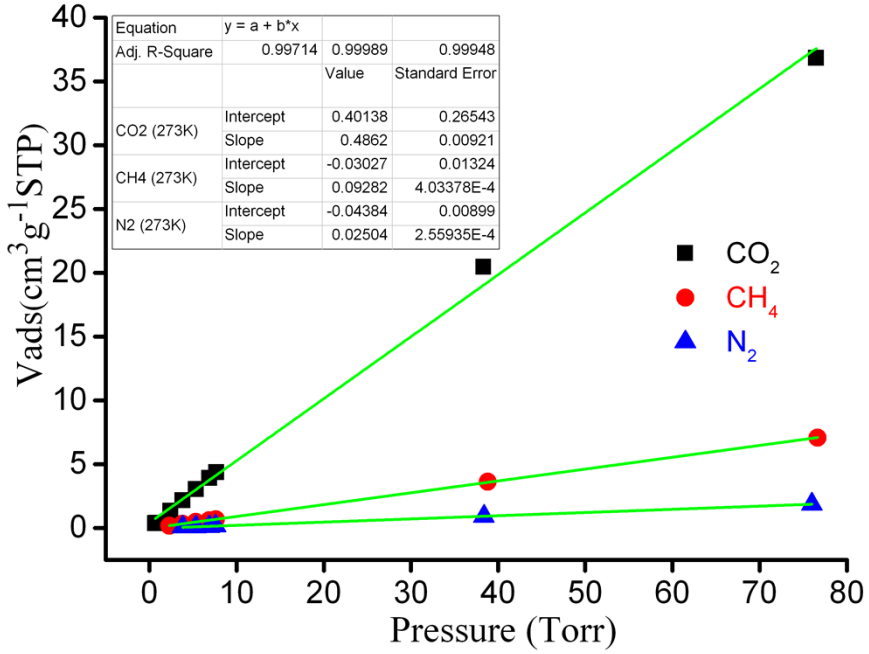

(a)

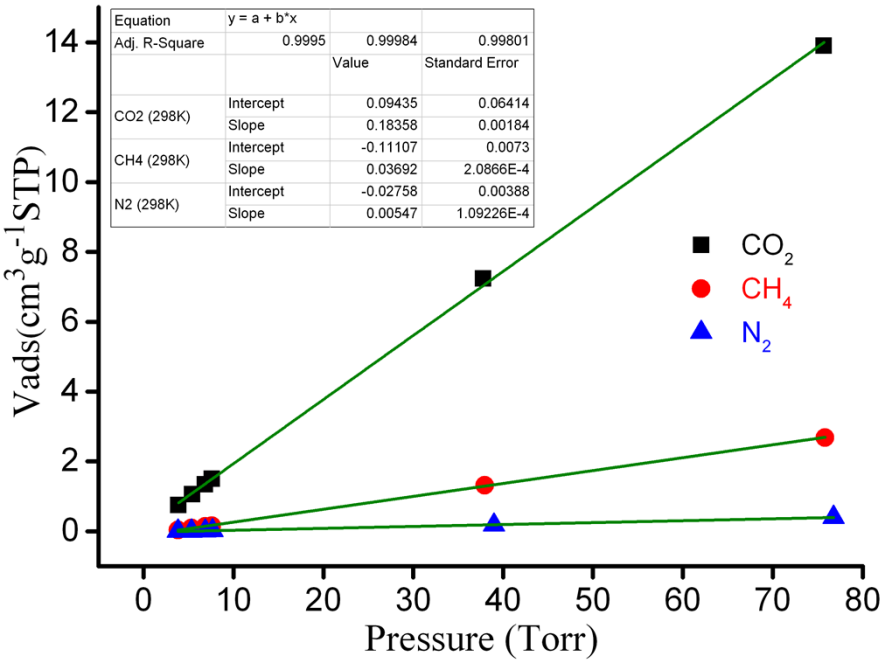

(b)

Figure S5 (a) The fitting initial slopes for CO_2, CH_4 and N_2 at 273 K. (b) The fitting initial slopes for CO_2, CH_4 and N_2 at 298 K.

Table S3. Summary of surface areas for **1** and other porous MOFs materials

MOF	surface area ($m^2 g^{-1}$) BET	Langmuir	Micropore volume ($m^3 g^{-1}$)	Percent of Void %	Ref
Complex **1**	905	1076	0.306	37.7	**This work**
UTSA-30	592	604	0.259	30.3	S4
UTSA-35	742.7	758.4	0.313	45.8	4b
PCN-100	371	860	0.58	80.8	S5
PCN-101	503	1140	0.75	—	S5
$[Zn_3(tcpt)_2(H_2O)_2]$	—	535	—	41.4	6
MOF-177	4500	5340	1.89	—	S6
JUC-113	—	132.6	—	—	5d
SNU-100	814	—	0.315	38.1	7
MOF-520	3290	3930	1.277	—	S7

Table S4. Summary of CO_2 and H_2 gas-adsorption data for MOFs in literature

MOF	CO_2 uptake ($cm^3 g^{-1}$)	Q_{st} of CO_2 ($kJ\ mol^{-1}$)	Selectivity (CO_2 / N_2)	H_2 uptake (Wt %)[d]	Q_{st} of H_2 ($kJ\ mol^{-1}$)	Ref
Complex **1**	71.3[a]	40.9-31.2	33.6[c]	2.19	8.10-7.11	**This work**
SNU-100'	71.7[a]	29.3-27.7	25.5[c]	1.81	8.14-7.08	7
SNU-100'-Mg	76.9[a]	36.3-34.9	32.6[c]	1.99	7.20-6.02	7
SNU-100'-Co	85.5[a]	37.4-36.4	40.4[c]	2.16	7.59-7.20	7
MOF-205-OBn	20.4[a]	16.5	16.5[c]	1.3	—	S8
MIL-101Cr-NH_2	80.64[a]	43-23	100[c]	—	—	S9
MIL-101Cr-NO_2	40.1[b]	—	17	—	—	S9
$[Zn_3(tcpt)_2(H_2O)_2]$	31.0[a]	31	—	1.02	7.3	6
MOF-177	17.3[a]	4	—	1.25	4.4	S6
BUT-11	53.1[a]	25.9-22.3	31.5[c]	—	—	S10
HKUST-1	100.8[a]	35	101[c]	—	—	S11
UTSA-30	33[a]	—	—	—	—	S4
ZIF-300	40[a]	—	22[c]	—	—	S12
ZIF-301	40[a]	—	19[c]	—	—	S12
ZIF-302	36[a]	—	17[c]	—	—	S12

MOF-649	—	—	—	0.7	5.3	S13
MOF-650	—	—	—	1.48	6.8	S13
PCN-101	—	—	—	0.47	—	S5
Cu_2(TPPC-O^{n}Hex)	—	—	—	1.48	6.22	S14
Cu_2(TPPC-O^{n}Pr)	—	—	—	1.96	7.22	S14
Fe_2(dobdc)	—	—	—	2.2	9.7	S15

[a]Obtained at 298 K and 1 atm. [b]Obtained at 293 K and 1 atm. [c]The calculated CO_2/N_2 selectivity from adsorption isotherms at 298 K. [d]Measured at 77 K and 1 atm.

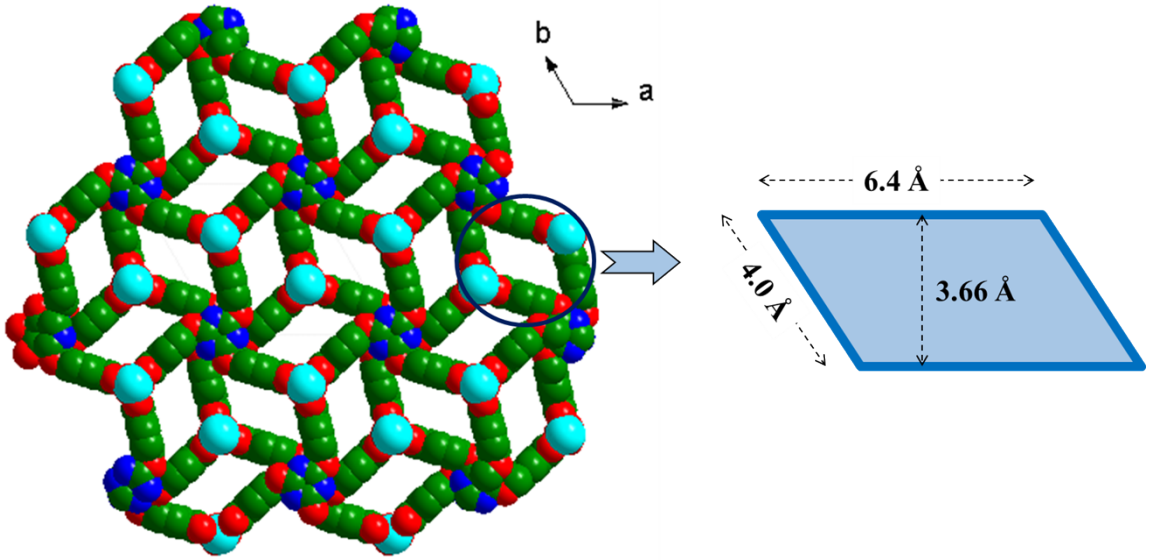

Figure S6 Pore size of the rhombic channels.

Solid ^{1}H NMR Study

As shown in figure S7, the two signals at δ=7.867, and 0.030 ppm can be assigned to the bridging hydroxyl groups and the aromatic CHs, respectively, while no signals of H_2O was observed around 4.5 ppm[S16].

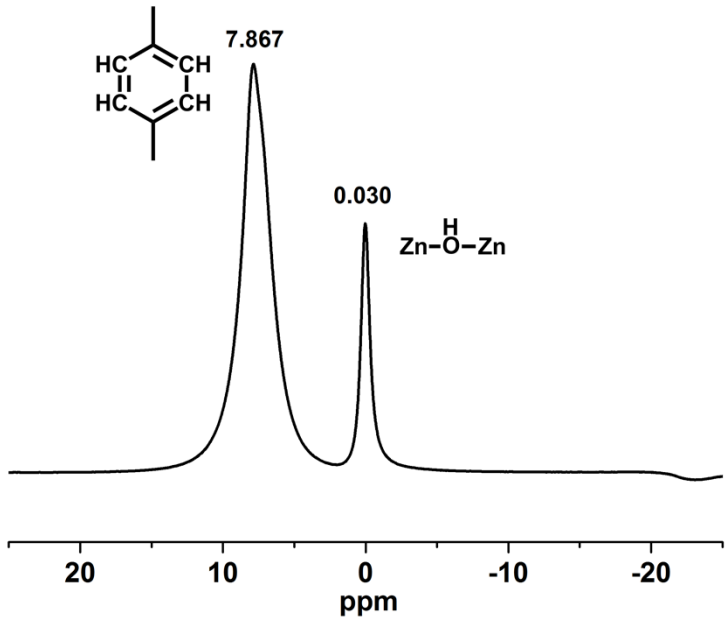

Figure S7 Solid ^{1}H NMR spectra for the degassed sample of **1**.

SI-Reference

[S1] L. Czepirski and J. JagieLlo, *Chem. Eng. Sci.*, 1989, **44**, 797.

[S2] A. Malek and S. Farooq, *AIChE J.*, 1996, **42**, 3191.

[S3] M. Dincă and J. R. Long, *J. Am. Chem. Soc.*, 2005, **127**, 9376.

[S4] Y. He, S. Xiang, Z. Zhang, S. Xiong, F. R. Fronczek, R. Krishna, M. O'Keeffee and B. Chen, *Chem. Commun.*, 2012, **48**, 10856.

[S5] Q.-R. Fang, D.-Q. Yuan, J. Sculley, J.-R. Li, Z.-B. Han and H.-C. Zhou, *Inorg. Chem*., 2010, **49**, 11637.

[S6] A. R. Millward and O. M. Yaghi, *J. Am. Chem. Soc*., 2005, **127**, 17998.

[S7] F. Gándara, H. Furukawa, S. Lee and O. M. Yaghi, *J. Am. Chem. Soc.*, 2014**, 136**, 5271.

[S8] J. Sim, H. Yim, N. Ko, S. B. Choi, Y. Oh, H. J. Park, S.Y. Park and J. Kim, *Dalton Trans*., 2014, **43**, 18017.

[S9] A. Khutia and C. Janiak, *Dalton Trans.*, 2014, **43**, 1338.

[S10] B. Wang, H. Huang, X.-L. Lv, Y. Xie, M. Li and J.-R. Li, *Inorg. Chem.*, 2014, **53**, 9254.

[S11] S. R. Caskey, A. G. Wong-Foy and A. J. Matzger, *J. Am. Chem. Soc*., 2008, **130**, 10870.

[S12] N. T. T. Nguyen, H. Furukawa, F. Gándara, H. T. Nguyen, K. E. Cordova and Omar M. Yaghi, *Angew. Chem. Int. Ed.*, 2014, **53**, 10645.

[S13] S. Barman, A. Khutia, R. Koitz, O. Blacque, H. Furukawa, M. Iannuzzi, O. M. Yaghi, C. Janiak, J. Hutter and H. Berke, *J. Mater. Chem. A*, 2014, **2**, 18823

[S14] T. A. Makal, X. Wang and H.-C. Zhou, *Cryst. Growth Des*., 2013, **13**, 4760.

[S15] W. L. Queen, E. D. Bloch, C. M. Brown, M. R. Hudson, J. A. Mason, L. J. Murray, A. J. Ramirez-Cuesta, V. K. Petersonc and J. R. Long, *Dalton Trans*., 2012, **41**, 4180.

[S16] T. Loiseau, C. Serre, C. Huguenard, G. Fink, F. Taulelle, M. Henry, T. Bataille and G. Férey, *Chem. Eur. J.*, 2004, **10**, 1373.